

An Efficient Hybrid Optimization Algorithm for Image Compression

Santosh Kumar B. P.

*YSR Engineering College of Yogi Vemana University,
Proddatur, Andhra Pradesh, India
bpsantoshkumar9@gmail.com*

Venkata Ramanaih K.

*YSR Engineering College of Yogi Vemana University,
Proddatur, Andhra Pradesh, India*

Abstract: In this work, a novel image compression approach is developed that is processed in several series of technologies. Here, the first process is the image segmentation and it is done using Adaptive ACM that partitions or segments the image into two regions such as ROI as well as non-ROI. Here, the adaptiveness of this ACM is determined with the idea of optimization algorithm. To handle the ROI regions, the JPEG-LS technique is exploited and to handle the non-ROI region the wavelet-based lossy compression technique is utilized. The outcome of both the JPEG-LS technique, as well as a wavelet-based compression approach is integrated with respect to the bit-stream amalgamation in order to produce the compressed image. Then, the compressed image is exploited to the image decompression that will be the overturn process of compression. It will comprise the bitstream separation that is subsequently individually process in both the wavelet-based decomposition and JPEG-LS decoding for obtaining the non-ROI regions and ROI. At last, the original image is obtained accurately. Moreover, the main objective of this paper falls in the adaptiveness under optimization. The maximum iteration and weighting factor in ACM are optimally chosen and for this a novel hybrid optimization technique is proposed, which hybridizes the concept of Differential Evolution method with Monarch Butterfly Optimization Algorithm. Here, the proposed method is compared with the conventional methods in order to shows its effectiveness for image compression.

Keywords: ROI; Image Compression; Lossless image; optimization; ACM

Nomenclature

Abbreviations	Descriptions
ACM	Adaptive Active Contour Model
CR	Compression Ratio
CT	Computed Tomography
MRI	Magnetic Resonance Imaging
STW	Spatial orientation Tree Wavelet
HEVC	High-Efficiency Video Coding
SPIHT	Set Partitioning in Hierarchical Trees
ROI	Region of Interest
TWT	Tree-structured Wavelet Transform
MED	Median Edge Detector
CS	Compressive Sensing
EZW	Embedded Zero trees of Wavelet transforms
WT	Wavelet Transform
VQ	Vector Quantization
DCT	Discrete Cosine Transform
MRP	Minimum Rate Predictors
WDR	Wavelet Difference Reduction
DWT	Discrete Wavelet Transform

1. Introduction

In current healthcare applications, the exploitation of medical imaging systems for diagnosis strategies is standard. In the past decades, with the development of digital systems and scanning approaches the aforesaid systems have become highly significant, creating more precise images with enhanced quality, exploiting bit depths and higher spatial resolutions. Such enhancements maximize the number of information, which requires to be transmitted, stored and processed. This is specifically suitable while

exploiting volumetric scanning approaches, such as MRI or CT, that create multiple image slices. MRI is a non-invasive imaging technology which produces three dimensional detailed anatomical images. It is frequently utilized for disease detection, diagnosis, and treatment monitoring. Moreover, CT is a noninvasive medical examination or procedure, which exploits specialized X-ray equipment to construct cross-sectional images of the body

In digital medical images, manipulation of enormous data is considered as the important issues. Their sizes create issues in visualization, transmission, interaction, and storage. In today's case, a cost-efficient approach to handle the digital medical images is especially vital to control the limitation in transmission; so here the only solution is compression [9]. Generally, compression is considered as the minimizing image size process without or with data loss. Several kinds of compressions are lossless, region-based and lossy compression [31].

In general, the reconstruction of the image without any data loss is performed by lossless compression. Nevertheless, the CR is minimum [10] when are not adequate for practical practices. The image information loss occurred due to lossy compression [11]. The loss of information tends to inaccurate diagnosis in medical images case. Nevertheless, few numbers of losses are tolerable based on the European Society of Radiology [12]. This varies for various medical images modality. In lossy compression of medical images, this standard aids within the bearable region. Both lossless and lossy compression approaches used by the region-based compression [13]. For near-lossless compression, the significant region of the image must be chosen to attain better-reconstructed image quality. Various research works are processing in order to develop the techniques for effectual segmentation the image to done region-based compression [6]. The segmentation techniques might maximize the difficulty of the complete compression process [29] [30].

Numerous approaches were developed to compress the images; however, the much demand revolution is the hybrid imaging approaches of that the VQ and DWT both of that are lossy compressions [14]. In functional and numerical analyses, a DWT is considered as a WT and that wavelets are discretely sampled, which is exploited for discrete-time signals processing [15]. The DCT worked on the basis of the cosine functions, the premises of DWT can be collected of any function, which fulfills the multiresolution analysis needs [17]. Adaptive transformations like bandelet [15] brushlet [14], and directionlet [16] need preceding information regarding the image. The fundamental function of these transforms alters based on the image content. Generally, in medical images, nonadaptive transforms are exploited to reduce complexity. In general, the WT based compression approach is exploited transformation approach due to its multi-resolution evaluation [18]. There are enormous wavelet-based compression approaches such as WDR [19], EZW [20] TWT [23], SPIHT [21], and STW [22].

This major objective of this article is to present a new compression model, which on the basis of the ROI. Moreover, the adaptiveness is concentrated in ACM as the optimization idea to obtain a precise outcome. Moreover, the maximum iteration and weighting factor in ACM are optimally chosen by a novel hybridization of Differential Evolution with Monarch Butterfly Optimization Algorithm, which have the ability to produce the compression task more precise.

2. Literature Review

In 2017, Saurin Parikh et al [1], proposes the exploitation of HEVC for diagnostically acceptable medical image compression, concentrating on compression effectual while comparing with the JPEG 2000. The problem of high bit-depth medical image compression and diagnostically acceptable lossy compression were examined.

In 2017, Luis F. R. Lucas et al [2], presented a highly effectual technique for lossless compression of volumetric sets for the medical images, like MRIs or CTs. The proposed technique indicated as 3D-MRP, which was on the basis of the principle of MRP that was considered as the conventional lossless compression techniques, stated in the data compression state-of-the-art.

In 2018, Jin Li et al [3], presented a novel heterogeneous CS technique for visible/near-infrared range. Unlike the existing CS approaches evenly allocating sensing resources, the presented technique completely uses texture-feature information for remote sensing images in order to aid the resources sensing allocation. Numerous sensing resources were allocated to high-frequency regions, however a smaller number of low-frequency regions.

In 2019, Paul Nii Tackie Ammah and Ebenezer Owusu [4], presented a DWT-VQ method to compress images and to protect their perceptual quality in a medically tolerant level. Here, salt and pepper and speckle and noises in ultrasound imagery were notably minimized. The process has a trivial effect, if the image was not ultrasound; however, the edge was preserved. Subsequently, the images were filtered exploiting DWT. By effectual means to produce the coefficients a threshold technique was exploited.

In 2019, J. Anitha et al [5], presented a lossy singular value and lossless prediction decomposition for the coefficients of ripplelet were performed to enhance the existing ripplelet transform-based system performance. At first, the prediction of lossless uses the correlation among the pixels of the image and alleviates the transformation process. Subsequently, the high and the low-frequency components were encoded by entropy model.

In 2018, K. Sheeba, and M. Abdul Rahiman [6] predicted an affine transformation in order to minimize the computational complexity. Moreover, the score value was also computed to further reduce the number of calculations in the comprehensive process of encoding. In this hybrid model, domain blocks and a relative geometric transformation of the range were identified by exploiting a reference matrix.

In 2019, Lihua Gong et al [7], presented effectual image encryption and compression technique on the basis of the compressive sensing and chaotic system. Initially, exploiting the Arnold transform original image permuted to minimize the block effect in the compression process, as well as subsequently the ensuing image was compressed and re-encrypted using compressive sensing, concurrently.

In 2017, S.Haddad et al [8], presented a novel joint watermarking-compression strategy the inventiveness of that represents the integration of the lossless compression conventional JPEG-LS with the bit interchange watermarking modulation. Without decompressing the image, this strategy permits access to watermarking-on the basis of the security services. It becomes probable to track images or to confirm their authenticity straightly from their compressed bitstream. The analysis of the proposed method stated with respect the embedding capacity and distortion and that were analyzed on ultrasound images.

3. Image Compression Approach using Adaptive Segmentation

In this work, a new image compression approach is developed, which is based on the ROI. At first, the proposed method utilizes Adaptive-ACM in order to partition the image into two regions such as non-ROI and ROI region. Moreover, to the ROI marked region, the JPEG-LS model is exploited to encode the non-ROI region, the wavelet-based lossy compression approach is exploited. Eventually the compressed image is attained.

Additionally, the decomposition process is the inverse process of compression. At first, the ROI mask code's bitstream is partitioned, which needs for decoding using the JPEG-LS decomposition technique. Also, the non-ROI code' is decompressed using the corresponding wavelet on the basis of the decompression technique. At last, the unique obvious region is restored efficiently. Since the presented method concentrates on precise outcome, the method is modelled to be robust regarding the Adaptiveness in ACM [24]. The adaptive idea is bit efficiently done with the integration of optimization idea. In ACM, maximum iteration and the weighting factor is optimally chosen using JCF-LA, which could be done the compression task accurate and efficient. Fig 1 demonstrates the block diagram of the developed technique.

3.1 Description of ACM

The preliminary development is considered as the image segmentation, whereas for segmenting the image, the active contour model is exploited. Moreover, the segmentation is based on both foreground and background, which defined regarding minimum local regions. Let us consider I_m as the stated input image, which is in the Δ domain. At first, the process initiates by fixing the maximum iteration MAX_{itr} . Moreover, C_c represents the closed contour, which stated as the "0" level set of ψ distance function specifically, $C_c = \{y | \psi(y) = 0\}$. The C_c interior is stated by the smoothed Heaviside function [24] which is stated in eq. (1). Then, the exterior C_c is decided as $(1 - F\psi(y))$. Moreover, a Dirac delta's smoothed version is exploited for recognizing the region around the curve, which is stated in eq. (2).

$$F\psi(y) = \begin{cases} 1, & \psi(y) < -\varepsilon \\ 0, & \psi(y) > \varepsilon \\ \frac{1}{2} \left\{ 1 + \frac{\psi}{\varepsilon} + \frac{1}{\pi} \sin\left(\frac{\pi\psi(y)}{\varepsilon}\right) \right\}, & \text{O.W} \end{cases} \quad (1)$$

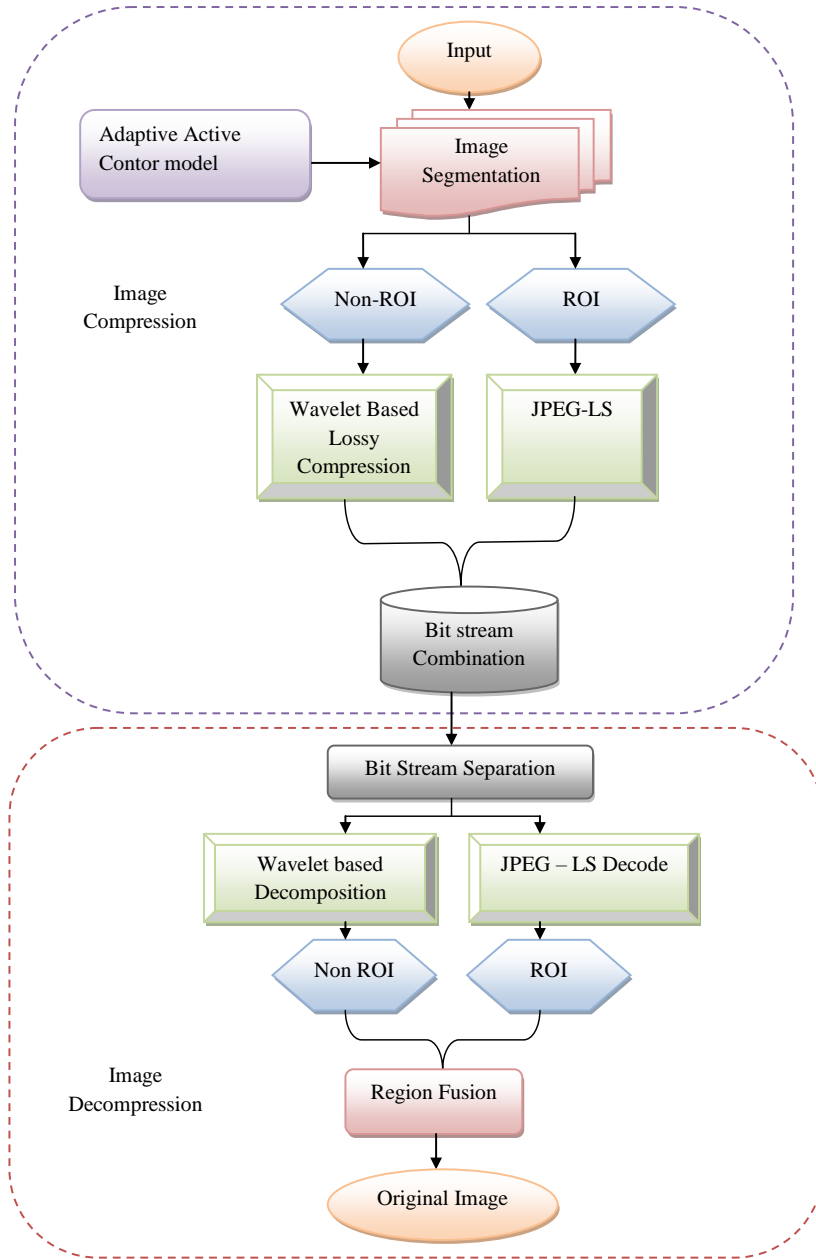


Fig. 1. Block diagram of the proposed model

$$\gamma\psi(y) = \begin{cases} 1, & \psi(y) = \varepsilon \\ 0, & |\psi(y)| < \varepsilon \\ \frac{1}{2\varepsilon} \left\{ 1 + \cos\left(\frac{\pi\psi(y)}{\varepsilon}\right) \right\}, & \text{O.W} \end{cases} \quad (2)$$

The method exploits spatial variables such as y and z as the characteristic spatial variables, which shows a single point in Δ . As in eq. (3) with these details, a feature function is developed regarding the radius parameters η . $M_s(y, z)$ is exploited to mask the local regions.

$$M_s(y, z) = \begin{cases} 1, & ||y - z| < \eta \\ 0, & \text{O.W} \end{cases} \quad (3)$$

Moreover, with the help of $M_s(y, z)$, an energy model, which is on the basis of the generic force model, F_N is stated as in eq. (4). The F_N model represents the generic internal energy measure, which exploited for denoting the local adherence.

$$E_N(\psi) = \int_{\Delta_y} \gamma\psi(y) \int_{\Delta_y} M_s(y, z) \bullet F_N(I(z), \psi(z)) dz dy \quad (4)$$

For maintaining the smooth curve, the augmentation of regularization phrase is performed. The arc length of the curves is weighted and penalized this penalty using ζ parameter (default value=0.2). The last energy is stated as eq. (5). The last evolution equation is shown in eq. (6) that is stated by considering the first deviation of energy regarding ψ .

$$E_N(\psi) = \int_{\Delta_y} \gamma\psi(y) \int_{\Delta_y} M_s(y, z) \bullet F_N(I(z), \psi(z)) dz dy + \xi \int_{\Delta_y} \gamma\psi(y) \|\nabla\psi(y)\| dy \quad (5)$$

$$\frac{\partial\psi}{\partial t} = \gamma\psi(y) \int_{\Delta_y} M_s(y, z) \bullet \nabla_{\psi(z)} F_N(I(z), \psi(z)) dz + \xi \delta\psi(y) \operatorname{div} \left(\frac{\nabla\psi(y)}{|\nabla\psi(y)|} \right) \quad (6)$$

The method partitions the image into two segments (as mentioned earlier) such as Non-ROI and ROI. The main objective of this paper is the adaptiveness in ACM technique. As mentioned before, fixing MAX_{itr} is the first process, as well as it plays a most important role in segmentation process. In this paper, this logic is optimized by choosing the optimal MAX_{itr} , which ranges from 100 to 500. Furthermore, for curve smoothing, the weighting factor ξ ranges from 0.1 to 0.5 is also made up to be optimized by the novel JCF-LA for obtaining enhanced outcomes.

3.2 JPEG-LS Lossless Image Compression Approach

By JPEG-LS technique, the ROI regions are handled [26] that is defined as follows: Under three basic steps such as Golomb-Rice coding, adaptive prediction, and context modelling, the method is processed. Moreover, the JPEG-LS predictor/modeller process the image in raster scan form with two function forms such as regular and run form. Specifically, for smooth region, the run form is coded in pixels the residual pixels are coded using regular form. To perform pixel coding y , at first the present x pixels is predicted through the MED that decides the gray values such as \hat{l}, \hat{m} and \hat{n} of 3 near pixels as stated in eq. (7).

$$\tilde{y} = \begin{cases} \min(\hat{l}, \hat{m}), & \hat{n} \geq \max(\hat{l}, \hat{m}) \\ \max(\hat{l}, \hat{m}), & \hat{n} < \min(\hat{l}, \hat{m}) \\ \hat{l} + \hat{m} - \hat{n}, & \text{O.W} \end{cases} \quad (7)$$

It is seen that the MED predictor is high efficient regarding the performance against other conventional predictors from the extensive assessment, and which is also concerned to be easy too. Then, the prediction continuing \hat{p} is increased by subtracting the attained predicted value from the current value, which is to encode that is stated in eq. (8).

$$\hat{p} = y - \tilde{y} \quad (8)$$

The pixel content is analyzed based on four pixels such as $\{\hat{l}, \hat{m}, \hat{n}, \hat{g}\}$. Moreover, the differences like $D_1^F = \hat{g} - \hat{m}$, $D_2^F = \hat{m} - \hat{n}$ and $D_3^F = \hat{n} - \hat{l}$ are also quantized. The local gradient is stated by the quantized differences; therefore the activity level in surrounding the pixel is captured, which manages the statistical behavior of the errors. In this technique, the total number of various contexts is 365. The error distribution for prediction is evaluated for each context exploiting prediction errors. Finally, \hat{p} refers prediction error as well as it is encoded by Golomb-Rice code using the model named context on the basis of the probabilistic method. Here \hat{e} refers the ranged at $[-2^{\hat{m}-1}, -2^{\hat{m}-1} - 1]$, in that \hat{m} refers to the pixel bit accuracy. In general, \hat{p} comprises geometric distribution (2-sided), which is almost certainly with a nonzero average value that evaluated and eradicated prior to performing the coding process using JPEG-LS's bias improvement. Moreover, using the interleaving positive and negative prediction error the geometric distribution (2-sided) is mapped into a 1-sided. Using the Golomb-Rice code, the efficient encoding of 1-side geometric distribution is performed.

3.3 Wavelet based Lossy Compression

In order to hold the non-ROI regions (blurred region) the Wavelet-based lossy compression [26] is exploited. An image is considered as the coefficient of 2D-array, as well as each coefficient represents the brightness level of that exacting point. On the whole, the natural images comprise smooth color variation, which possesses well details represented as sharp edges amongst the smooth variations. In scientific, the smooth deviation in color is indicated as low-frequency deviation, as well as the representation of sharp deviation is represented as maximum frequency deviation. Here, under

minimum frequency, the components comprise the image base, and with maximum frequency, the components are augmented upon them in order to refine the image, hence the detailed image can be obtained. Therefore, the smooth variations are extremely insistent than the details. Then, the smooth deviation and the image details would be done by the image decomposition through DWT.

In DWT, the minimum and maximum pass filters are selected consequently that they precisely bisect the range of frequency among them. The process initiates with offering the minimum pass filter for each data row.

At last, the attained outcomes from wavelet-based lossy compression and JPEG-LS technique are integrated for attaining the compressed image. Likewise, the decompression is also done; in that way without losing the quality of the image, the original image is reconstructed.

4. Hybrid Optimization Algorithm for Image Compression

4.1 Conventional DE Algorithm

The conventional DE technique is an easy but strong search approach [27], as well as it is exploited in order to solve the complex continuous nonlinear models. The conventional DE method begins with initializing a N_m population target individuals $M^t = \{y_1^t, y_2^t, \dots, y_{N_m}^t\}$, whereas t indicates the current iteration, individual $y_i^t = (y_{i,1}^t, y_{i,2}^t, \dots, y_{i,n}^t)$, $i = 1, 2, \dots, N_m$ is an t -dimensional vector with parameter values decided arbitrarily. The crossover, as well as mutation operators, are used to produce new candidate vectors, and a chosen strategy is exploited to decide whether the parent or the off-spring exist to the subsequent generation. The aforesaid process is continued until a stop condition is attained. There are numerous mutation schemes in state-of-the-art works [35]. Eq. (9) states the basic operator used in many works.

$$U_i^t = y_t^{\text{best}} + SF(y_a^t - y_d^t) \quad (9)$$

In eq. (9) a, d represents two arbitrarily selection registers in the range $[1, N_m]$ and $SF \in [0, 1]$ represents a scaling factor of mutation.

4.2 Conventional Monarch Butterfly Optimization Algorithm (MBFA)

The MBFA is the latest optimization algorithm that imitates the migration capability of the monarch [28]. Here, the butterfly migrates on Land 1 and Land 2, by the immigration, they generate their offspring. Correspondingly, in two manners, the locations of the monarch butterflies are updated. Initially, by the migration operator, the off-springs are produced. Then, the locations of the other butterfly modify operator tunes the butterflies. Additionally, the butterfly modifying operator and migration operator has exploited concurrently.

For Land 1 and 2, the population is partitioned into two sub-populations. $N_{m_1} = \text{ceil}(m * N_m)$ and $N_m - N_{m_1}$ indicates the number of monarch butterflies in Land 1 and Land 2, correspondingly. Moreover, $\text{ceil}(y)$ rounds y to the closer integer higher than or equal to y ; N_m indicates the population size; m indicates the monarch butterflies ratio in Land 1 and set to 5/12.

The arbitrary step walks dy on the basis of the Levy flight eq. (11) is augmented to motivate the exploration and exploitation process of the MBFA technique. Eq. (10) denotes the update j^{th} monarch butterfly exploited the arbitrary step walk dy .

$$y_{j,k}^{t+1} = y_{j,k}^{t+1} + \beta(dy_k - 0.5) \quad (10)$$

dy represents the walk step of butterfly j which is stated in eq. (6), and computed by exploiting Levy flight [7]. In eq. (12), β represents the weighting factor by setting the W_{\max} , which represents the max walk step.

$$dy = \text{levy}(y_j^t) \quad (11)$$

$$\beta = \frac{W_{\max}}{t^2} \quad (12)$$

Regarding the migration behavior of the monarch butterfly individuals, the MBFA technique can be created, as well as its diagrammatic illustration can be explained in the below steps.

4.3 Description of Proposed model

To enhance the convergence capability of conventional DE as well as MBFA, a new hybridization of MBFA and DE is proposed. In this proposed method, two methods are hybrids, such as MBFA and DE. Here, MBFA with a crossover method from DE as an adaptation is developed in this paper. The MBFA performance enhances while integrating it with DE. In the conventional MBFA method, the M population is partitioned into M_1 as subpopulation 1 and M_2 as subpopulation 2 at each generation t . In DE- MBFA, a novel population of mutant monarch butterflies U is augmented on the basis of the eq. (9) to enhance the quality of the solution. Since in conventional MBFA, the novel population U is partitioned into two subpopulations $U1_i \in U, i = 1, \dots, N_{m_1}$ and $U2_j \in U, j = N_{m_1} + 1, \dots, N_m$.

By formulating with idealizing the MBFA Migration process, the recently created monarch butterflies in Land 1 for Subpopulation 1 are produced on the basis of the chosen of monarch butterflies from M_1 as well as M_2 . Nevertheless, in the proposed algorithm migration process, the novel M_1 is produced by choosing the monarch butterflies from M_1 and V_2 .

In this work, the MBFA, the Butterfly is modified by adjusting operator. The objective of the Butterfly modifying operator is to idealize the process of exploitation as well as exploration and evade any possible traps in the local minima in the complete search. To perform that, eq. (10) is altered using eq. (13).

$$y_{j,k}^{t+1} = y_{avg}^t + dy_{j,k}^t \quad (13)$$

In eq. (13), the present monarch butterfly updating is changed from $y_{j,k}^t$ to y_{avg}^t , whereas, y_{avg}^t represents the average of the monarch butterflies in Subpopulation 2, and it is represented in eq. (14).

$$y_{avg}^t = \left(\frac{1}{N_{m_2}} \sum_{j=1}^{N_{m_2}} y_{j,1}^t, \dots, \frac{1}{N_{m_2}} \sum_{j=1}^{N_{m_2}} y_{j,n}^t \right) \quad (14)$$

As demonstrated in Eq. (13), the Levy flight is modified using a new presented step size dy . dy of the j^{th} monarch butterfly is computed using eq. (15).

$$dy_{j,k}^t = \beta * rn * 10v_{j,k}^t \quad (15)$$

In eq. (15) β is indicated using Eq. (12), rn represents a normally distributed arbitrary number, as well as $v_{j,k}^t$ represents an integer arbitrary number among 1.0 to 6.0 produce at every decision variable k of each j^{th} monarch butterfly.

As stated in the conventional MBFA, the newly produced monarch butterflies in Land 2 for subpopulation 2 are produced on the basis of the chosen of the monarch butterflies from the Subpopulation 2 and optimal solution. In the proposed method, the newly produced monarch butterflies M_2 are chosen from the optimal solution and U_2 . On the basis of the modifying rate of butterfly BR is adjusted in the presented method and it is computed using eq. (16).

$$BR^t = \Delta \left(1 - \frac{t}{\max_{itr}} \right) \quad (16)$$

In eq. (16), \max_{itr} represents the utmost iteration number, t represents the present iteration, as well as the parameter, Δ is chosen. The parameter BR is linearly minimizing from Δ to 0 by maximizing the numeral of generations. Here, to enhance the solution quality by exploiting the novel walk step for the monarch butterfly dy in eq. (15) as well as the novel parameter BR .

Initiating with $BR = \Delta$, the search space is investigated to observe for the best solutions, to minimize the BR value, and to use the search space. In Land 2, the monarch butterflies are not merely updated from y_{best} and U_2 , other than as well as a novel parameter γ is added to offer the mutant monarch butterfly U_1 of Land 1 a possibility for migration. It is observed that the MBFA method can balance the migration operator direction by modifying the ratio m . By the proposed DE-MBFA, two of modifying the ratios, m_1 and m_2 , are generated for the butterfly modifying and migration operator, correspondingly. Here, m_1 is set equal to m in MBFA, whereas $m_1 = 5/12$, and $m_2 = 0:02$. Moreover, the value m_2 is chosen to be minimizing in order to decrease the likelihood of falling into a local minimum. If m_2 is high, more elements from the monarch butterflies in the current optimal solution will be chosen. Additionally, the parameter γ is set on the basis of the work as 0.1; it indicates the selection form U_1 is lesser than or equal to 10% of the whole population. Fig 2 demonstrates the detailed description of proposed DE-MBFA model.

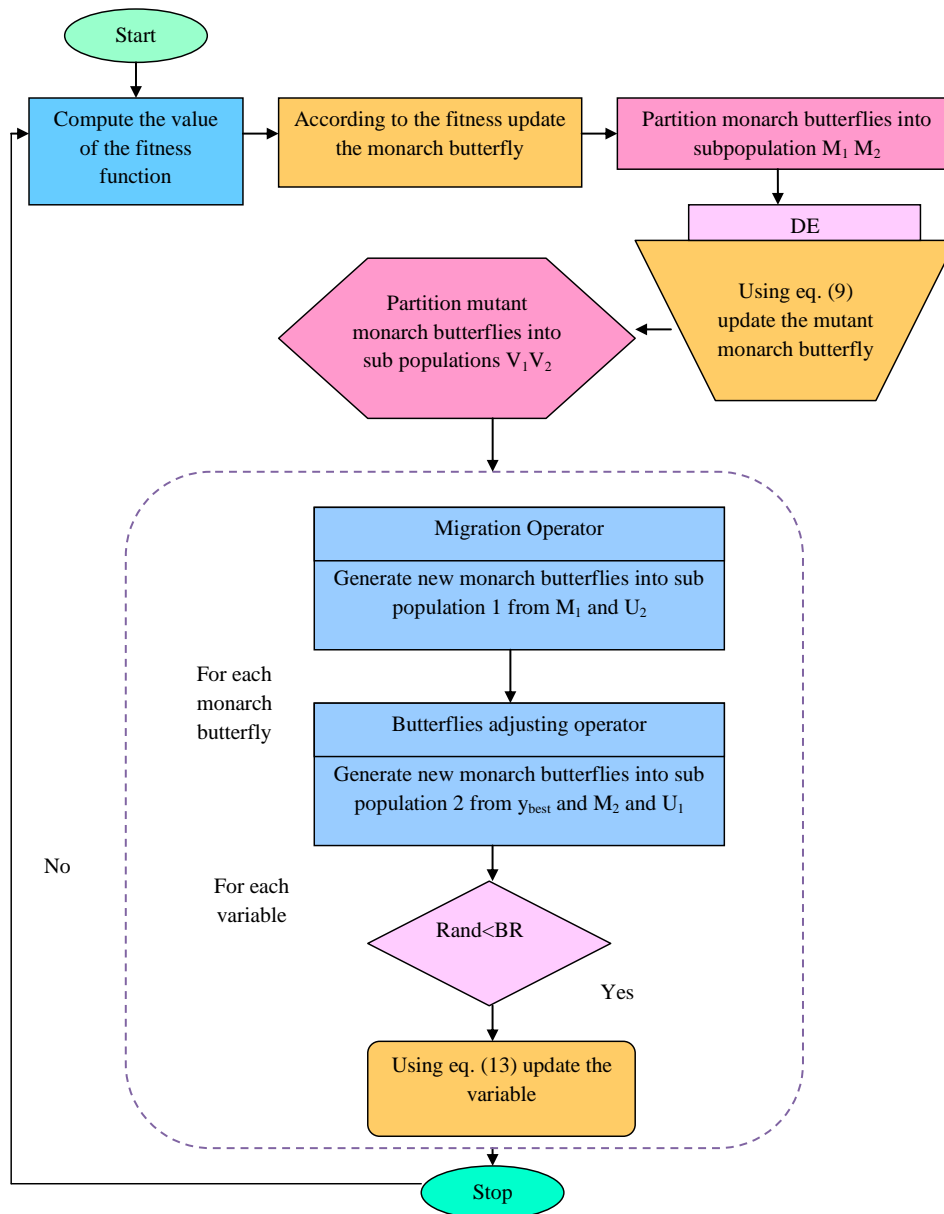


Fig. 2. Flow diagram of the proposed model

5. Results and Discussions

5.1 Experimental Procedure

In MATLAB 2018 a, the presented image compression technique experimented. For the simulation analysis, images are obtained from BRATS database (<https://www.smir.ch/BRATS/Start2015#7s8d6f87>). The proposed model was compared with the existing models like Differential Evolution (DE), Butterfly Optimization (BFO), and Genetic Algorithm (GA) methods regarding Accuracy, Specificity, Sensitivity, Precision, False Negative Rate (FNR), False Positive Rate (FPR), False Discovery Rate (FDR) F1_Score, Net Present Value (NPV), and Matthews's correlation coefficient (MCC).

5.2 Performance Evaluation

For the proposed algorithm, the analysis of the CR is performed regarding two scenarios such as handling of non-ROI by wavelet-based algorithm and handling of ROI by JPEG-LS algorithm, which is shown in Fig 3 and 4. Generally, the ratio of the compression decides the compressed original image as well as image size ratio that should be minimized in fact without the loss of quality of the image. Eq. (17) states the mathematical formula of CR.

$$\text{Compression ratio} = \frac{\text{Size of Compressed Image}}{\text{Size of Original Image}} \tag{17}$$

Fig 3 exhibits the performance analysis of the proposed model over conventional algorithms such as DE, BFO, and GA. Here, the proposed method is analyzed over the five cases such as best, worst, median, mean, and Standard Deviation (SD) based on ROI using JPEG-LS. In the best-case, the developed method achieves minimum CR, and it is 25.12%, 23.12%, and 22% superior to the conventional DE, BFO and GA algorithms.

Fig 4 demonstrates the performance analysis of the proposed method over conventional techniques like DE, BFO, and GA. Here, the proposed method is evaluated over the five scenarios such as best, worst, median, mean, and SD based on NROI using the wavelet-based algorithm. In the best case, the developed method attains the minimum ratio of the compression, and it is 31.23%, 29.29%, and 28.33% superior to the conventional DE, BFO and GA algorithms.

Table 1 states the performance analysis of the proposed approach with the existing techniques with respect to the positive and negative metrics. The accuracy of the proposed method is 12% better than the DE, 23% better than the BFA, and 28% better than the GA algorithms. From Table 1, it is proved that the proposed technique is effectual regarding the accurate image compression without losing its information.

Table 1. Performance analysis of the proposed method over conventional methods

Measure	DE	BFA	GA	Hybrid DE- MBFA
Accuracy	0.72345	0.86578	0.86790	0.98346
Sensitivity	0.43534	0.45456	0.45236	0.056222
Specificity	0.92343	0.95678	0.83345	0.99278
FPR	0.10769	0.085612	0.17231	0.046818
Precision	0.10523	0.10589	0.098765	0.099195
FDR	0.88762	0.89008	0.90174	0.90321
MCC	0.16747	0.10001	0.18048	0.035922
FNR	0.76124	0.75362	0.34462	0.94326
NPV	0.89481	0.91686	0.79234	0.99125
F1_score	0.12456	0.14567	0.13492	0.051227

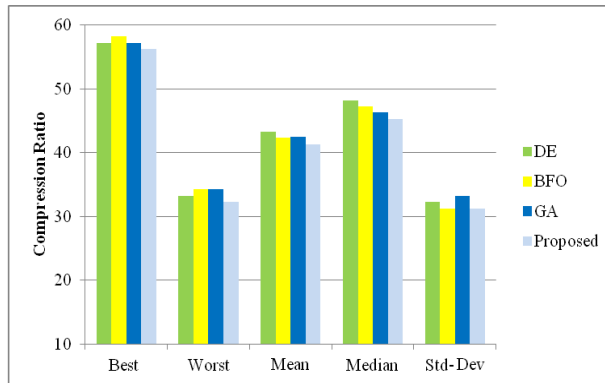


Fig. 3. Analysis of CR for the proposed technique on the basis of ROI by JPEG-LS

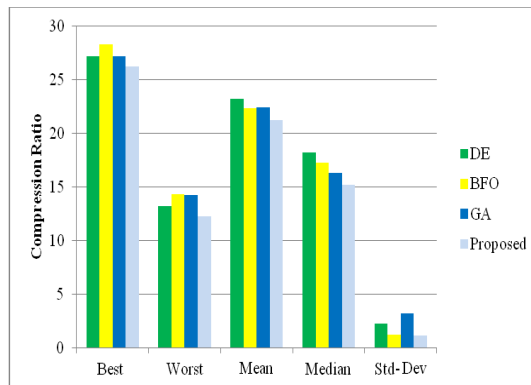


Fig. 4. Analysis of CR for the proposed technique on the basis of Non-ROI by the wavelet-based approach

6. Conclusion

This work presents a novel image compression technique with various sequences of process. At first, ACM is used exploited to perform the segmentation process which segments the image into two divisions. Here, the JPEG-LS method is exploited to the marked ROI regions, as well as the wavelet-based lossy compression method are exploited to encode the non-ROI region. The result from both wavelet-based compression model and JPEG-LS technique are integrated regarding the bit-stream combination and produce the compressed image. Additionally, the reverse process to obtain the original image is performed. The ACM is integrated with the adaptive idea through the optimization is considered as the main objective. Moreover, the maximum iteration and weighting factor of ACM is optimally chosen using a novel DE- MBFA technique. At last, the presented method is compared to other existing techniques regarding several measures. Therefore, the presented model is shown to be efficient regarding the effectual image compression with less error rate.

References

- [1] S. S. Parikh, D. Ruiz, H. Kalva, G. Fernández-Escribano and V. Adzic, "High Bit-Depth Medical Image Compression With HEVC," *IEEE Journal of Biomedical and Health Informatics*, vol. 22, no. 2, pp. 552-560, March 2018.
- [2] L. F. R. Lucas, N. M. M. Rodrigues, L. A. da Silva Cruz and S. M. M. de Faria, "Lossless Compression of Medical Images Using 3-D Predictors," in *IEEE Transactions on Medical Imaging*, vol. 36, no. 11, pp. 2250-2260, Nov. 2017.
- [3] J. Li, Y. Fu, G. Li and Z. Liu, "Remote Sensing Image Compression in Visible/Near-Infrared Range Using Heterogeneous Compressive Sensing," in *IEEE Journal of Selected Topics in Applied Earth Observations and Remote Sensing*, vol. 11, no. 12, pp. 4932-4938, Dec. 2018.
- [4] Paul Nii Tackie Ammah, Ebenezer OwusuRobust medical image compression based on wavelet transform and vector quantization", *Informatics in Medicine Unlocked*, Volume 15, 2019, Article 10018.
- [5] J. Anitha, P. Eben Sophia, Le Hoang Son, Victor Hugo C. de Albuquerque, "Performance enhanced ripplelet transform based compression method for medical images", *Measurement*, Volume 144, October 2019, Pages 203-213.
- [6] K. Sheeba, M. Abdul Rahiman, "Gradient based fractal image compression using Cayley table", *Measurement*, Volume 140, July 2019, Pages 126-132.
- [7] Lihua Gong, Kaide Qiu, Chengzhi Deng, Nanrun Zhou, "An image compression and encryption algorithm based on chaotic system and compressive sensing", *Optics & Laser Technology*, Volume 115, July 2019, Pages 257-267.
- [8] S. Haddad, G. Coatrieux, M. Cozic, D. Bouslimi, "Joint Watermarking and Lossless JPEG-LS Compression for Medical Image Security", *IRBM*, Volume 38, Issue 4, August 2017, Pages 198-206.
- [9] Francois G. Meyer, Ronald R. Coifman, Brushlets: a tool for directional image analysis and image compression, *Appl. Comput. Harmon. Anal.* 4 (1997) 147– 187.
- [10] Erwan Le Pennec, Stéphane Mallat, Sparse geometric image representations with bandelets, *J. Mag.* C1614 (4) (2005) 423–438.
- [11] Vladan Velisavljevic, Baltasar Beferull-Lozano, Martin Vetterli, Pier Luigi Dragotti, Directionlets: anisotropic multi-directional representation with separable filtering, *IEEE Trans. Image Process.* 15 (7) (2006) 1916–1933.
- [12] P.P.S.A. Reboucos Filho, V.M.N. Peixoto, D.J. Raul, G.M. Hemanth, A.K. Aldisio, C. de A. SangiahVicto Hugo, Automatic histologically closer classification of skin lesions, *Comput. Med. Imag. Graph.* 68 (2018) 40–54.
- [13] B. Kaur, M. Sharma, M. Mittal, A. Verma, L.M. Goyal, D.J. Hemanth, An improved salient object detection algorithm combining background and foreground connectivity for brain image analysis, *Comput. Elect. Eng.* 71 (2018) 692–703.
- [14] Spaulding J, Noda H, Shirazi MN, Kawaguchi E. BPCS steganography using EZW lossy compressed images. *Pattern Recognition Letters* 2002;23:1579-1587.
- [15] Mallat SG. A Theory for Multiresolution Signal Decomposition: The Wavelet Representation. *IEEE Transactions on Pattern Analysis and Machine Intelligence* 1989;11:674-693.
- [16] Vetterli M, Herley C. Wavelets and Filter Banks: Theory and Design. *IEEE Transactions on Signal Processing* 1992;40.
- [17] Daubechies I. *Ten Lectures on Wavelets*, Society for Industrial and Applied Mathematics. Philadelphia; 1992.
- [18] P.P.S.A. Reboucos Filho, V.M.N. Peixoto, D.J. Raul, G.M. Hemanth, A.K. Aldisio, C. de A. SangiahVicto Hugo, Automatic histologically closer classification of skin lesions, *Comput. Med. Imag. Graph.* 68 (2018) 40–54.
- [19] Y. Yuan, M.K. Mandal, Novel embedded image coding algorithms based on wavelet difference reduction, *IEE Proc.-Vis., Image Sig. Process.* 152 (2005) 9–19.
- [20] J.M. Shapiro, Embedded image coding using Zerotrees of Wavelet Coefficients, *IEEE Trans. Image Process.* 41 (12) (1993) 3445–3462.
- [21] A. Said, W.A. Pearlman, A new fast and efficient image codec based on set partitioning in hierarchical trees, *IEEE Trans. Circuits Syst. Video Technol.* 6 (3) (1996) 243–250.
- [22] A. Said, W.A. Pearlman, Image compression using the spatial-orientation tree, *IEEE Int. Symp. Circuits Syst.*, Chicago, IL 1 (1993) 279–282.

- [23] A. Adhipathi Reddy, B.N. Chatterji, Texture image compression using tree structured wavelet transform, IETE J. Res. 50 (1) (2004) 63–67.
- [24] Meyer-Bäse A, Jancke K, Wismüller A, et al. Medical image compression using topology-preserving neural networks. Eng Appl Artif Intell. June 2005;18(4):383–392.
- [25] Parikh SS, Ruiz D, Kalva H, et al. High bit-depth medical image compression with HEVC. IEEE J Biomed Health Inform. March 2018;22(2): 552–560.
- [26] Okumura A, Suzuki J, Furukawa I, et al. Signal analysis and compression performance evaluation of pathological microscopic images. IEEE Trans Med Imaging. Dec. 1997;16(6):701–710.
- [27] Z. Gao, Z. Pan and J. Gao, "A New Highly Efficient Differential Evolution Scheme and Its Application to Waveform Inversion," in IEEE Geoscience and Remote Sensing Letters, vol. 11, no. 10, pp. 1702-1706, Oct. 2014.
- [28] G. Wang, X. Zhao and S. Deb, "A Novel Monarch Butterfly Optimization with Greedy Strategy and Self-Adaptive," 2015 Second International Conference on Soft Computing and Machine Intelligence (ISCMI), Hong Kong, 2015, pp. 45-50.
- [29] Vinusha S,"Secret Image Sharing and Steganography Using Haar Wavelet Transform "Multimedia Research, Volume 1, Issue 1, October 2018.
- [30] Vinolin V and Vinusha S,"Edge-based Image Steganography using Edge Least Significant Bit (ELSB) Technique "Multimedia Research, Volume 2, Issue 2, October 2018.
- [31] A Rega, A Mennitto, S Vita, L Iovino,"New technologies and autism: can augmented reality (ar) increase the motivation in children with autism" 12th International Technology, Education and Development Conference,4904-4910.